Cellular and Molecular Biology

Research Article Open Access

Cation-dependent Mannose 6-Phosphate Receptor Functions as a Key Regulator of Palmitic Acid-induced Cell Death in Cardiomyocytes

Qiaoli Zeng[1,3,4], Xiaoyi Xu[2,4], Taili Yang[3,6], Hengli Zhang[3,6],Taotao Shao[3,6], Bing Tan[3,5], Zhaoshou Yang[5*] and Runmin Guo[1,3,6]

[1]*Department of Internal Medicine, Shunde Women and Children's Hospital (Maternity and Child Healthcare Hospital of Shunde Foshan), Guangdong Medical University, Foshan 528300, Guangdong, China*

[2]*Guangzhou Laboratory, Guangzhou International Bio Island, Guangzhou, China*

[3]*Key Laboratory of Research in Maternal and Child Medicine and Birth Defects, Guangdong Medical University, Foshan 528300, Guangdong, China*

[4]*State Key Laboratory of Ophthalmology, Zhongshan Ophthalmic Center, Sun Yat-sen University, Guangdong Provincial Key Laboratory of Ophthalmology and Visual Science, Guangzhou 510060, Chin*

[5]*The First Affiliated Hospital/School of Clinical Medicine of Guangdong Pharmaceutical University, Guangdong Pharmaceutical University, Guangzhou, Guangdong 510080, P.R. China*

[6]*Department of endocrinology, Affiliated Hospital of Guangdong Medical University, Zhanjiang 524000, Guangdong, China*

Abstract

Background: Palmitic acid (PA), a common saturated free fatty acid, is known as inducer of apoptosis in numerous cell types. M6PR-CD has been reported as a potential pro-apoptotic factor in several models.

Objective: We aim to identify the critical regulatory molecules in the process of palmitate-induced apoptosis in H9C2 cardiomyocytes.

Methods: Cells treated with 250 μM PA for 24 hours were collected. Transcriptome sequencing and bioinformatics analysis were carried out to screen the differentially expressed genes. RT-PCR and western blot were used to confirm the up-regulation of M6PR-CD. The function of M6PR-CD was studied through the detection of cell viability, apoptosis and intracellular ROS levels.

Results: A total of 1025 differentially expressed genes were screened by transcriptome sequencing, including 718 up-regulated genes and 307 down-regulated genes. Gene Ontology (GO) and Kyoto Encyclopedia of Genes and Genomes (KEGG) analysis were mainly focused on the apoptotic and stress. M6PR-CD was significantly up-regulated with PA treatment. Knockdown of M6PR-CD alleviated the PA-induced apoptosis with lower ROS levels. After transfection with M6PR-CD siRNA, it was also found that compensatory increase in M6PR-CI subtype did not exist, and the expression of caspase-3 was almost the same.

Conclusion: This study identified a number of genes related to PA-induced cardiomyocytes apoptosis through transcriptome sequencing. It was clarified for the first time that M6PR-CD could induce H9C2 cardiomyocytes apoptosis by enhancing ROS production rather than being Caspase-3-dependent, providing a theoretic basis for us to have a better understanding of the intrinsic mechanism.

Keywords: M6PR-CD; Palmitic acid; Cardiomyocytes; Cell death

Introduction

The decrease in the number of cardiomyocytes caused by apoptosis is one of the main reasons why cardiac function declines. At present, it has been recognized that cardiomyocyte apoptosis played a significant role in the pathogenesis of many cardiovascular diseases, including congestive heart failure, myocardial infarction, ischemia reperfusion damage, myocarditis and cardiomyopathy. Although many important signaling molecules and pathways were reported to be involved in cardiomyocyte apoptosis, the processes have not yet been fully elucidated [1].

Excessive lipid accumulation in non-adipose tissue will cause cell dysfunction. In a variety of myocardial diseases, the abnormal fatty acid metabolism will lead to the accumulation of toxic lipid metabolism intermediates. They can inhibit the activity of the enzyme system and induce the aggregation of reactive oxygen species (ROS) that trigger cell apoptosis [2]. A large number of cell and animal models in the heart have confirmed that the imbalance of lipid intake and utilization can induce programmed apoptosis of cardiomyocytes [3-6]. It has also been proven that a high concentration of palmitate acid can promote apoptosis in different types of cardiomyocytes [7, 8]. In this study, transcriptome sequencing was used to find key regulatory molecules in the model of PA-induced apoptosis of H9C2 cells, aiming to identify new targets for treating myocardial diseases.

Mannose 6-phosphate receptor (M6PR), mainly distributed on the Trans surface of Golgi complex and the plasma membrane, have two subtypes: cation-dependent mannose 6-phosphate receptor, M6PR-CD (46 kDa) and cation-independent mannose 6-phosphate receptor, M6PR-CI (300 kDa) [9, 10]. The ability of the two receptors to bind mannose 6-phosphate (Man-6-P) is basically the same [11]. The former preferentially transports lysosomal enzymes with one Man-6-P residue, while the latter tends to transport two [12, 13]. At present, there are many researches on M6PR-CI. M6PR-CI is involved in the activation of TGFβ1 protein and participates in the degradation of leukemia inhibitory factor (LIF) [14]. It can combine with mannos-6-phosphory pentene and induce protein to be hydrolyzed and activated [15]. The

***Corresponding author:** Zhaoshou-Yang, The First Affiliated Hospital/School of Clinical Medicine of Guangdong Pharmaceutical University, Guangdong Pharmaceutical University, Guangzhou, Guangdong 510080, P.R. China, E-mail: yangzhsh3@gdpu.edu.cn

Received: 01-Oct-2023, Manuscript No: cmb-23-115244; **Editor assigned:** 04-Oct-2023, PreQC No: cmb-23-115244(PQ); **Reviewed:** 18-Oct-2023, QC No: cmb-23-115244; **Revised:** 25-Oct-2023, Manuscript No: cmb-23-115244(R); **Published:** 30-Oct-2023, DOI: 10.4172/1165-158X.1000291

Citation: Zeng Q, Xu X, Yang T, Zhang H, Shao T, et al. (2023) Cation-dependent Mannose 6-Phosphate Receptor Functions as a Key Regulator of Palmitic Acid-induced Cell Death in Cardiomyocytes. Cell Mol Biol, 69: 291.

functions of two subtypes are similar but different. For example, a lack of M6PR-CI will disturb the lysosomal function more greatly than a lack of M6PR-CD [16]. The M6PR-CD deficient mice can survive but fail to sort the hydrolases properly in serum and urine, while the one lacking M6PR-CI usually overgrow in the embryonic period and die in the perinatal period because of the accumulation of IGF-II [17, 18]. Furthermore, M6PR-CD can negatively regulate the process of APP and the production of Aβ, while M6PR-CI can positively regulate the process of APP and the production of Aβ [19]. In this study, the up-regulation of M6PR-CD was observed in cells treated with PA. However, little is known about what role M6PR-CD plays in myocardial disease. The impact of M6PR-CD on cardiomyocyte apoptosis has also remained unclear.

Materials and Methods

CCK-8 detection

The cell line H9C2 was obtained from Procell (Wuhan, China). H9C2 cells were maintained in DMEM supplemented with 10 % FBS and 1 % antibiotics (penicillin-streptomycin). Palmitic acid (PA, Sigma) was dissolved in 0.15M KOH solution. The stock solution of PA (50 mM) was diluted to different final concentrations in the DMEM containing 0.5 % BSA. Cells were seeded in 96-well plates at a density of 10, 000 cells per well and respectively treated with PA for 4, 8, 12 and 24 hours. 10μL CCK8 was added to each well and the mixture was incubated for two hours. The absorbance was read with a microplate reader at 450 nm.

Detection of apoptosis rate and ROS

Cells were seeded in 24-well plates at a density of 50, 000 cells per well and treated with 250 μM PA for 24 hours. The same volume of KOH solution was added to the control group. Subsequently, cells were respectively stained using the apoptosis kit (KeyGEN BioTECH, KGA106) and reactive oxygen species kit (Beyotime, NO. S0033S). The flow cytometry (BD FACS Aria II) was used to detect fluorescence signal for the analysis of apoptotic cell rate and intracellular ROS levels.

Transcriptome sequencing

Agilent 2100 bioanalyzer was used to detect the integrity and total amount of RNA. Then the first and second strands of cDNA were synthesized through mRNA with polyA tail gathered by Oligo (dT) magnetic beads. AMPure XP beads were used to screen about 370-420 bp cDNA. PCR amplification was carried out, and the PCR product was purified with AMPure XP beads. Then the library was diluted to 1.5 ng/μl, whose effective concentration was accurately quantified by RT-qPCR (the effective concentration of the library was higher than 2 nM) to ensure the quality of the library. According to the effective concentration and the demand of target offline data, Illumina sequencing was performed and 150 bp paired terminal readings were generated. The image data of the sequenced segment detected by the high-throughput sequencer was converted into sequence data (reads) after CASAVA base recognition. In order to ensure the quality and reliability of data analysis, it was necessary to filter the original data, including the removal of reads with adapter, reads that cannot determine base information, and low-quality reads (the number of bases with Qphred ≤ 20 accounts for more than 50 %). In addition, the content of Q20, Q30 and GC in clean data was calculated. All subsequent analysis were high-quality and based on clean data.

Differential expression analysis

DESeq2 software (1.20.0) was used to analyze the difference expression between the two groups. DESeq2 provided statistical procedures to determine differential gene expression based on the model of negative binomial distribution. Benjamini and Hochberg methods were used to adjust the P value to control the rate of false discovery. When $p < 0.05$, the genes were identified as differentially expressed genes.

Differential gene enrichment analysis

ClusterProfiler (3.4.4) software was used to analyze the statistical enrichment of differentially expressed genes in the GO and KEGG pathway. Considering the GO term with a corrected P value less than 0.05, the gene length deviation was corrected through significant enrichment of differentially expressed genes, including biological process, cellular component and molecular function. KEGG was a database resource, which was used to understand the advanced functions of biological system.

RT-qPCR

Cells were seeded in 24-well plates at a density of 50, 000 cells per well and treated with 250 μM PA for 24 hours. Total RNA was isolated using RNA rapid extraction kit (Accurate Biology, AG21023) and cDNA was synthesized using reverse transcription kit (Accurate Biology, AG11728). Then RT-qPCR was carried out with SYBR Green qPCR Mix (Beyotime, D7260). The following primer sequences were used: M6pr-CD, forward: 5′- TGATTGTCCCTTGTGTGGGA-3′, reverse: 5′-GGCTAGCGAGACTACCACAAG-3′; β-actin, forward: 5′-GGCTGTATTCCCCTCCATCG-3′, reverse: 5′-AACACAGCCTGGATGGCTAC-3′.

Small molecule interference M6PR-CD

The M6PR-CD siRNA and negative control siRNA were purchased from Tsingke Biotechnology (Beijing, China). The target sequence of siRNA for M6PR-CD was GGAAGTAACTGGATCATGT. The sequences of M6PR-CD siRNA include 5'- GGAAGUAACUGGAUCAUGUTT-3' and 5'- ACAUGAUCCAGUUACUUCCTT-3'. H9C2 cells were seeded into 35 mm culture dish at a density of 6×105 cells/ mL. All siRNAs were transfected to cells using RNAi-Mate (Genepharma, Shanghai, China). Transfected cells were cultured for 36 hours before further experiments. RT-qPCR and western blot were used to assess the efficiency of siRNA knock-down.

Statistical analysis

All data were expressed as mean ± SEM. The differences between two groups were analyzed by unpaired two tailed t-test using GraphPad Prism 8 (GraphPad Software, USA). When there were two variables, one way analysis of variance or two way analysis of variance combined with Tukey's comparation test were used. P values were expressed as $^{*}p < 0.05$, $^{**}p < 0.01$ and $^{***}p < 0.001$ respectively. When $p < 0.05$, the differences were considered statistically significant.

Results

Palmitic acid promotes cardiomyocyte apoptosis

CCK8 detection was carried out at 4 hr, 8 hr, 12 hr and 24 hr after adding different concentrations of PA (125 μM, 250 μM and 500 μM). It was shown that cell viability decreased in a time-dose dependent manner after treatment with PA (Figure 1A). Furthermore, treating H9C2 cells with 250 μM PA for 24 hours could significantly increase the level of ROS (Figure 1B) and the rate of apoptosis cells (Figure 1C).

Differentially Expressed Proteins in PA-treated H9C2 Cells

Compared with the control group, a total of 1025 differentially

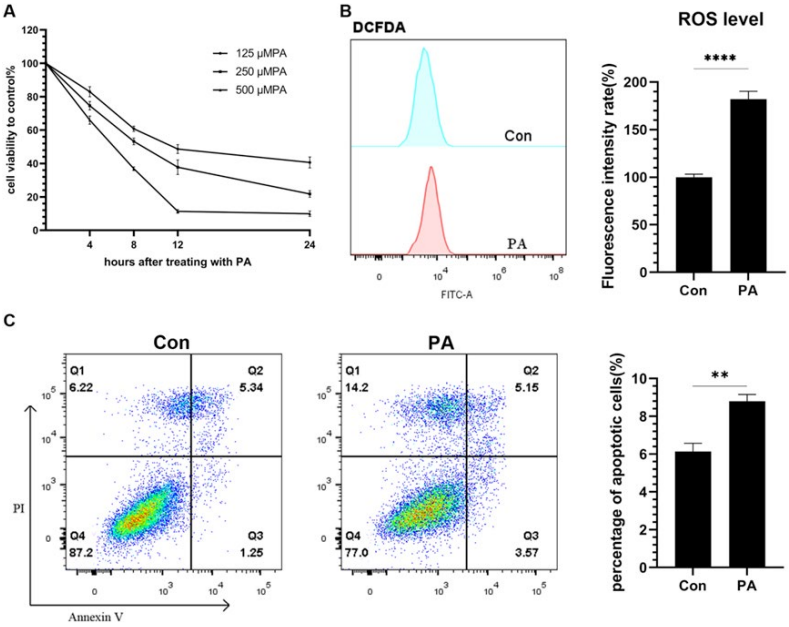

Figure 1: Palmitic acid can promote cardiomyocyte apoptosis. (A) H9C2 cells were respectively incubated with 125, 250 and 500 μM PA for 4, 8, 12 and 24 h. Cell viability was measured using the CCK8 assay. (B) After exposure to 250 μM PA for 24 hours, H9C2 cells were respectively stained with PI/Annexin FITC and DCFH-DA probe. Flow cytometric analysis of apoptotic cell rate (B) and intracellular ROS level (C) were conducted.

expressed genes were identified in the PA group, among which 718 genes were up-regulated and 307 genes were down-regulated. The filter criteria included |log2 (Fold Change) | > 1 and $p \leq 0.05$. In the volcano map, red dots represented up-regulated genes and green dots represented down-regulated genes (Figure 2A). In the cluster analysis, the redder the color is, the higher the gene FPKM is. Similarly, the greener the color is, the lower the gene FPKM is. In conclusion, there was a significant difference between PA group and control group (Figure 2B).

GO and KEGG analysis

Among the up-regulated genes, GO analysis can be classified into biological process, cellular component, and molecular function. Biological process analysis mainly concentrates on intrinsic apoptotic signaling pathway in response to endoplasmic reticulum stress, endoplasmic reticulum unfolded protein response, negative regulation of megakaryocyte differentiation and so on; The enrichment of cellular component mainly includes ribosome, cytosolic ribosome, and cytosolic part; Molecular function mainly occurs in structural constituent of ribosome and receptor ligand activity (Figure 3A). KEGG mainly focuses on Ribosome, Systemic lupus erythematosus, Ferroptosis, and Apoptosis (Figure 3B). Correspondingly, among the down-regulated genes, biological processes mainly concentrate on positive regulation of toll-like receptor signaling pathway, regulation of double-strand break repair via homologous recombination, cellular response to alcohol; Cellular component focuses on anchored component of synaptic membrane, intrinsic component of presynaptic active zone membrane, myosin complex; Molecular function mainly includes transmembrane signaling receptor activity, purinergic nucleotide receptor activity, nucleotide receptor activity (Figure 3C). KEGG pathways of down-regulated genes mainly contains antigen processing and presentation, hypertrophic cardiomyopathy, protein digestion, absorption, and toll-like receptor signaling pathway (Figure 3D).

PA induces up-regulation of M6PR-CD transcription

The mRNA transcriptome sequencing showed that M6PR-CD was significantly up-regulated in PA group (|log2 Fold Change| = 3.0851 and $p = 0.000205456$) (Figure 4A). Further, after 250 μM PA treatment for 24 hours, RT-qPCR was used to confirm the up-regulation of M6PR-CD in PA group ($p < 0.01$), which was consistent with mRNA sequencing results (Figure 4B); Western blot also confirmed the up-regulation of M6PR-CD (Figure 4C).

M6PR-CD promotes cardiomyocyte apoptosis

Transfection with M6PR-CD siRNA successfully suppressed the expression of M6PR-CD mRNA (Figure 5A) and protein (Figure 5B). It is observed that compensation did not exist between the M6PR-CD and M6PR-CI subtypes (Figure 5C). The knockdown of M6PR-CD blocked PA-induced death in H9C2 cells, which improved cell viability (Figure 5D) and decreased the rate of apoptotic cells (Figure 5E, 5F). In addition, exposure of H9C2 to PA led to higher ROS production, while transfection with M6PR-CD siRNA could prevent the increase of ROS generation (Figure 5G). However, caspase-3 protein level did not change in the transfected cells (Figure 5C). These results suggest that M6PR-CD could promote cell apoptosis by enhancing the formation of ROS, which is independent of the activation of caspase-3.

Discussion

In this study, we employed transcriptome sequencing to identify a number of regulatory molecules relevant to cardiomyocyte apoptosis in the model of PA-induced apoptosis in H9C2 cells. Among up-regulated differentially expressed genes, GO analysis can be classified into biological process, cellular component, and molecular function. Biological processes mainly gather in the intrinsic apoptotic signaling pathway in response to endogenous reticulum stress, and endogenous reticulum unfilled protein response, etc. It has been reported that PA

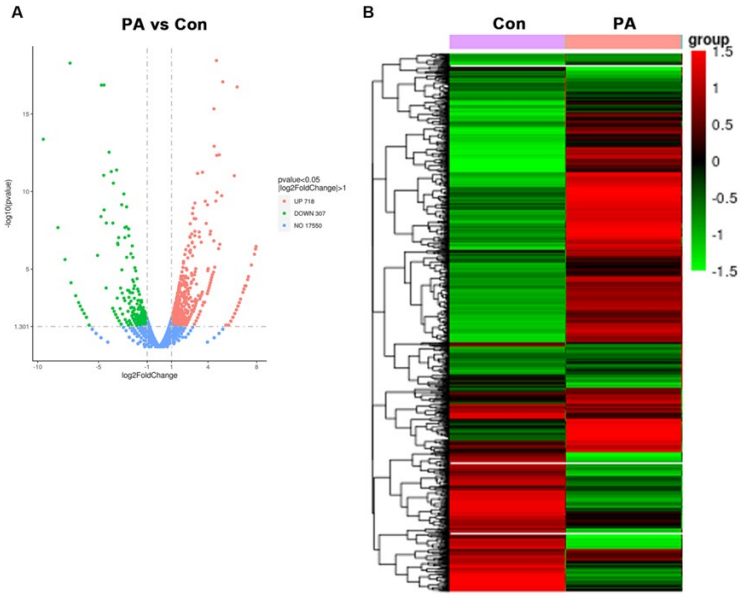

Figure 2: Screening differentially expressed genes by transcriptome sequencing. (A) The horizontal axis of the volcano map represents the fold change of gene expression (log2 Fold Change), and the vertical coordinate represents the significant level of gene expression difference (-log10 p value). Up-regulated genes are represented by red dots, and down-regulated genes are represented by green dots. (B) In the cluster analysis, the horizontal axis represents the sample name, while the vertical coordinate represents the normalized value of the gene FPKM. The redder the color is, the higher the count of gene expression is. The greener the color is, the lower the count of gene expression is.

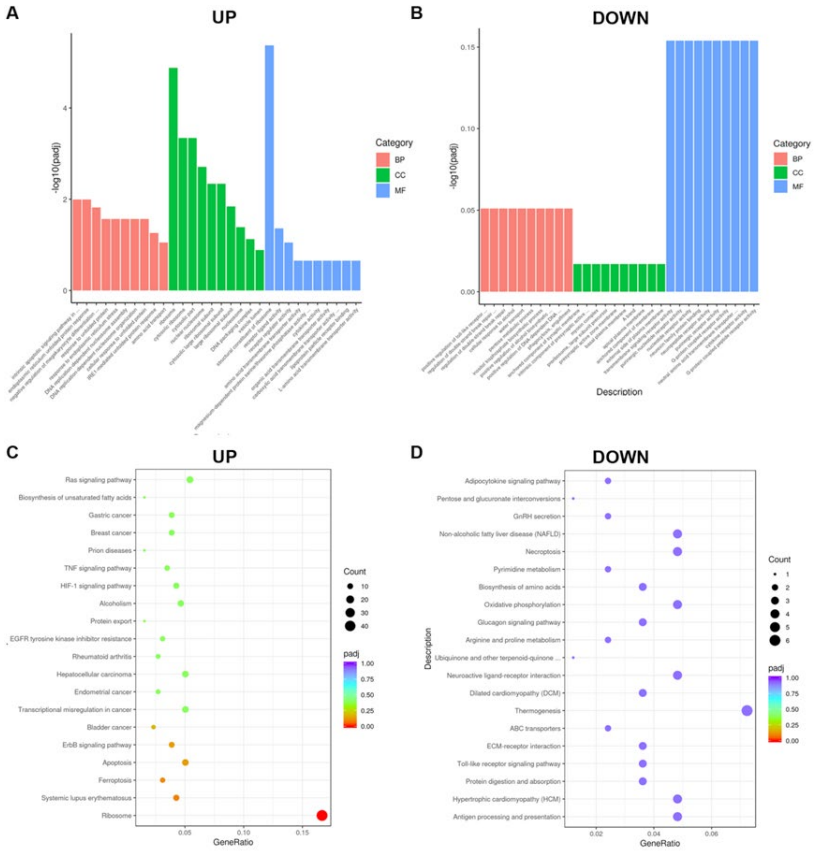

Figure 3: GO and KGEE analysis of differentially expressed genes. Use clusterProfiler (3.4.4) software to analyze GO (including Biological process, Cellular component and Molecular function) (A, B) and KGEE pathway (C, D) among up-regulated and down-regulated genes respectively.

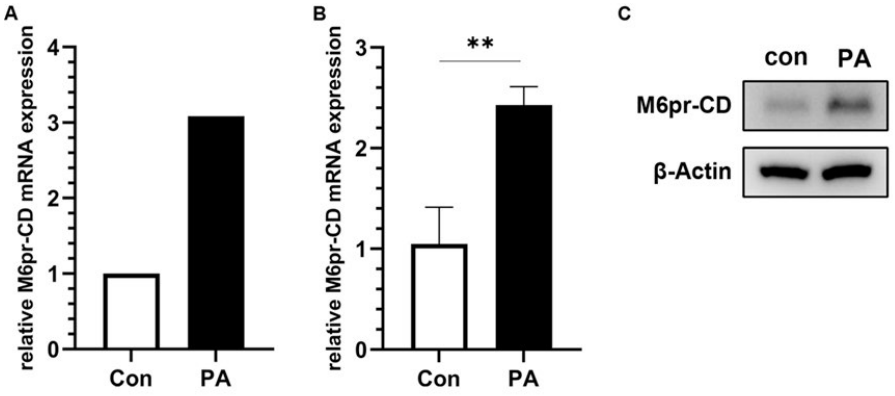

Figure 4: PA can induce up-regulation of M6PR-CD. (A) Transcriptome sequencing analyzes the fold change of M6PR-CD. After H9C2 cells were treated with 250 μM PA for 24 hours, the expression of M6PR-CD were detected by PCR (B) and Western blot (C).

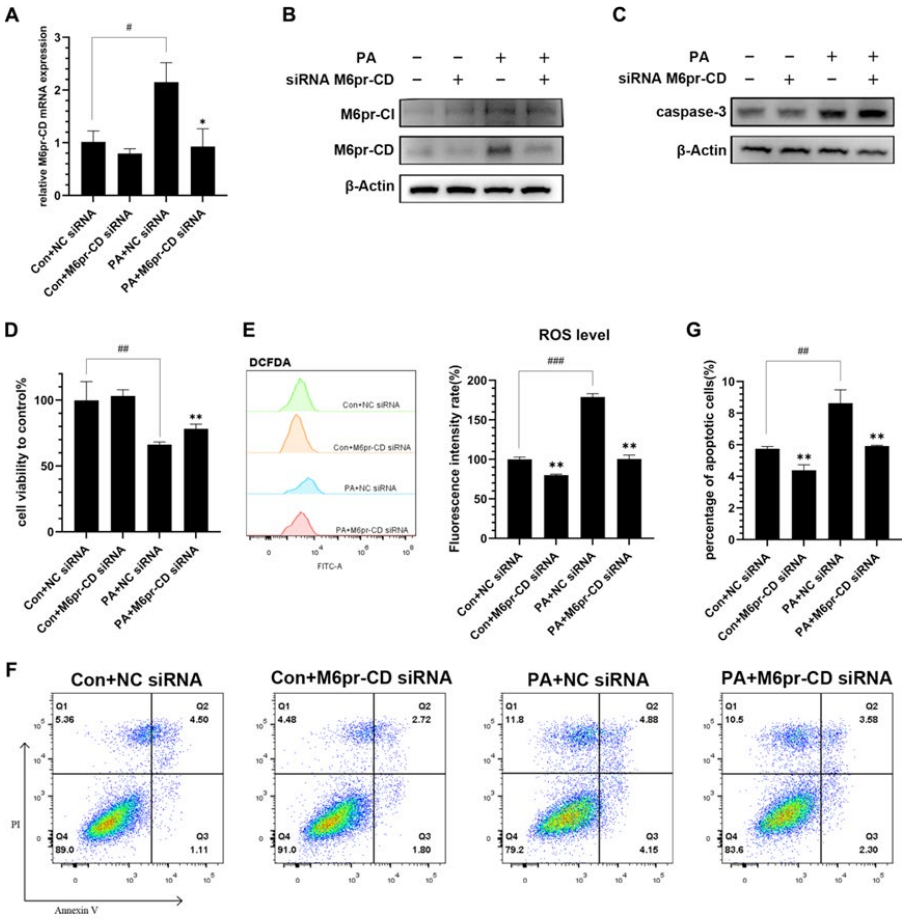

Figure 5: M6PR-CD can enhance the generation of ROS to induce cardiomyocyte apoptosis. (A) After transfection with M6PR-CD siRNA or negative control siRNA, H9C2 cells were treated with 250 μM PA for 24 hours. PCR was used to assess the efficiency of M6PR-CD knock-down. Western blot was used to analyze the expression of M6PR-CD, M6PR-CI (B) and caspase-3 protein (C). (D) CCK8 detected the change of cell viability. (E) Cells were stained with DCFH-DA probe, and flow cytometry was used to analyze ROS level. (F,G) Cells were stained with annexin V-FITC/PI, and flow cytometry was used to analyze apoptotic cell rate.

could hinder the shape and integrity of the endoplasmic reticulum by increasing the saturated fatty acid content, resulting in endoplasmic reticulum stress and apoptosis [20]. PA can also induce the mitochondria of H9C2 cells to release cytochrome c and promote the expression of apoptosis signal molecules, such as BAX, cleaved caspase-3, and cleaved PARP [21]. Besides, PA can aggravate inflammation by enhancing the activation of CCAAT enhancer binding protein, which is induced by unfilled protein response. Molecular function is primarily enriched in receptor ligand activity, etc. PA can mediate the activation of EGFR via TLR4/c-Src, resulting in myocardial inflammation and hypertrophy. Purine receptor P2X7R is also involved in PA-induced apoptosis of H9C2 cells. KEGG analysis mainly focuses on ferroptosis and apoptosis. It is stated that PA can trigger ferroptosis by suppressing the generation of glutathione peroxidase 4 (GPX4) and enhancing the production of ACSL4 [22-26].

As for down-regulated differential genes, the biological processes mainly concentrate on the positive regulation of toll like receptor signaling pathway, regulation of double strand break repair via homologous recombination, etc. Previous research has established that PA could directly bind to MD2 to activate TLR4 and downstream inflammatory reactions, such as TLR4/MyD88/NF-κB signal pathway [27, 28]. PA can also impair mitochondrial DNA (mtDNA), while overexpression of hOGG1 in mitochondria can protect mtDNA from damage [29]. The molecular function is mainly enriched in the transmembrane signaling receptor activity, purinergic nucleotide receptor activity, etc. Overexpression of GPR40 can rescue the PA-mediated myocardial damage via SIRT1/LKB1/AMPK pathway [30]. KEGG analysis mainly includes protein digestion and absorption. PA stimulates the DRP1 protein to translocate from cytoplasm to mitochondria, causing mitochondrial damage and cell dysfunction [31]. PA also induces lipotoxicity in H9C2 cells and converts CD36-mediated energy metabolism to GLUT4-mediated energy metabolism [32]. In conclusion, PA can trigger cardiomyocyte death through varieties of mechanisms, including endoplasmic reticulum stress, cell apoptosis, ferroptosis, mitochondrial DNA damage, TLR4 receptor activation, etc [7, 33, 34].

Besides, it is widely accepted that apoptosis is closely related to lysosomal system disorders [35], in which M6PR plays an important role. In this study, the up-regulation of M6PR-CD was observed in the PA group through transcriptome sequencing. Furthermore, our study has identified, for the first time that M6PR-CD could promote cell apoptosis by boosting the generation of ROS. M6PR has two subtypes, M6PR-CD and M6PR-CI. The two receptors have complementary functions in lysosomal enzyme targeted transport. It has previously been observed that the ability of two receptors to transport newly synthesized lysosomal enzymes was similar, but the efficiency of binding with targeted ligands was different. In double-negative fibroblasts, overexpression of M6PR-CD only partially corrected lysosomal enzyme transport, while overexpression of M6PR-CI completely reversed the dislocation of lysosomal enzyme [36]. Targeted destruction of M6PR-CD in mice led to lysosomal protein transduction errors. In the M6PR-CD deficient mice, the level of phosphorylated lysosomal enzymes increased significantly in the extracellular fluid. Moreover, the phenotype of M6PR-CD deficient mice was normal, and the expression of M6PR-CI did not change, suggesting that the lack of M6PR-CD cannot be compensated by M6PR-CI [17, 37].

Currently, most of research focuses on the role of M6PR-CI in myocardial disease, while very little is known about M6PR-CD. M6PR-CI can activate Gαq-mediated signal pathway, leading to the increased expression of key proteins in cardiac hypertrophy [38, 39]. M6PR-CI can also down-regulate the expression of survival protein p-Akt, p-Bad and enhance the expression of apoptosis related protein. In addition, Doxorubicin treatment can increase the amount of M6PR-CI in heart tissue and promote cardiomyocyte apoptosis, while CREB overexpression will inhibit hypoxia-induced M6PR-CI and reduced H9C2 cell apoptosis. The apoptosis of H9C2 cells can also be blocked by M6PR-CI antibody and calcineurin inhibitor CsA. The research above reveals that M6PR-CI can induce cardiomyocytes apoptosis. However, the association between M6PR-CD and cardiomyocytes apoptosis is still unclear. Our study demonstrates for the first time that M6PR-CD is also involved in the pathogenesis of cardiomyocyte apoptosis by promoting the production of ROS [40-42].

Conclusion

In the model of PA-induced H9C2 cardiomyocyte apoptosis, it was observed that M6PR-CD expression was up-regulated, and there was no compensatory increase in M6PR-CI subtype. In addition, M6PR-CD promoted cardiomyocyte apoptosis by enhancing ROS generation rather than activating caspase-3.

Data Availability

The datasets used or analyzed during the current study are available from the corresponding author on reasonable request.

Conflicts of Interest

The authors have no conflicts of interest to declare.

Acknowledgements

This work was supported by grants from the National Natural Science Foundation of China (No. 81873649) and the Medical Research Project of Foshan Municipal Health Bureau (20210188and20210289); Guangdong Medical University Research Foundation (GDMUM2020008 and GDMUM2020012);. Science and Technology Program of Guangzhou (202103000051).

References

1. Chen ZH, Na HK, Hurh YJ, Surh YJ (2005) 4-Hydroxyestradiol induces oxidative stress and apoptosis in human mammary epithelial cells: possible protection by NF-kappaB and ERK/MAPK. Toxicol Appl Pharmacol 208: 46-56.
2. Dyntar D, Eppenberger-Eberhardt M, Maedler K, Pruschy M, Eppenberger H, et al. (2001) Glucose and palmitic acid induce degeneration of myofibrils and modulate apoptosis in rat adult cardiomyocytes. Diabetes 50: 2105-2113.
3. Pillutla P, Hwang YC, Augustus A, Yokoyama M, Yagyu H, et al. (2005) Perfusion of hearts with triglyceride-rich particles reproduces the metabolic abnormalities in lipotoxic cardiomyopathy. Am J Physiol Endocrinol Metab 288:1229-1235.
4. Chiu HC, Kovacs A, Blanton RM, Han X, Courtois M, et al. (2005) Transgenic expression of fatty acid transport protein 1 in the heart causes lipotoxic cardiomyopathy. Circ Res 96: 225-233.
5. Cheng L, Ding G, Qin Q, Huang Y, Lewis W, et al. (2004) Cardiomyocyte-restricted peroxisome proliferator-activated receptor-delta deletion perturbs myocardial fatty acid oxidation and leads to cardiomyopathy. Nat Med 10: 1245-1250.
6. Cheng L, Ding G, Qin Q, Huang Y, Lewis W, et al. (2004) Cardiomyocyte-restricted peroxisome proliferator-activated receptor-delta deletion perturbs myocardial fatty acid oxidation and leads to cardiomyopathy. Nat Med 10: 1245-1250.
7. Zou L, Li X, Wu N, Jia P, Liu C, et al. (2017) Palmitate induces myocardial lipotoxic injury via the endoplasmic reticulum stressmediated apoptosis pathway. Mol Med Rep 16: 6934-6939.
8. Li C, Liu Z, Xu Q, Peng H, Cao J, et al. (2021) PXDN reduces autophagic flux in insulin-resistant cardiomyocytes via modulating FoxO1. Cell Death Dis 12: 41-81.
9. Saftig P, Klumperman J (2009) Lysosome biogenesis and lysosomal membrane

proteins: trafficking meets function. Nat Rev Mol Cell Biol 10: 623-35.

10. Motyka B, Korbutt G, Pinkoski MJ, Heibein JA, Caputo A, et al. (2000) Mannose 6-phosphate/insulin-like growth factor II receptor is a death receptor for granzyme B during cytotoxic T cell-induced apoptosis. Cell 103: 491-500.
11. Kornfeld S (1992) Structure and function of the mannose 6-phosphate/ insulinlike growth factor II receptors. Annu Rev Biochem 61: 307-30.
12. Munier-Lehmann H, Mauxion F, Hoflack B, et al. (1996) Function of the two mannose 6-phosphate receptors in lysosomal enzyme transport. Biochem Soc Trans 24: 133-136.
13. Ahmed KA, Xiang J (2017) mTORC1 regulates mannose-6-phosphate receptor transport and T-cell vulnerability to regulatory T cells by controlling kinesin KIF13A. Cell Discov 3: 170-181.
14. Blanchard F, Duplomb L, Raher S, Vusio P, Hoflack B, et al. (1999) Mannose 6-Phosphate/Insulin-like growth factor II receptor mediates internalization and degradation of leukemia inhibitory factor but not signal transduction. J Biol Chem 274: 24685-24693.
15. Leksa V, Ilkova A, Vicikova K, Stockinger H (2017) Unravelling novel functions of the endosomal transporter mannose 6-phosphate/insulin-like growth factor receptor (CD222) in health and disease: An emerging regulator of the immune system. Immunol Lett 190: 194-200.
16. Sohar I, Sleat D, Gong Liu C, Ludwig T, Lobel P, et al. (1998) Mouse mutants lacking the cation-independent mannose 6-phosphate/insulin-like growth factor II receptor are impaired in lysosomal enzyme transport: comparison of cation-independent and cation-dependent mannose 6-phosphate receptor-deficient mice. Biochem J 330: 903-908.
17. Koster A, Saftig P, Matzner U, von Figura, Peters C, et al. (1993) Targeted disruption of the M(r) 46,000 mannose 6-phosphate receptor gene in mice results in misrouting of lysosomal proteins. EMBO J 12: 5219-23.
18. Lau MM, Stewart CE, Liu Z, Bhatt H, Rotwein P, et al. (1994) Loss of the imprinted IGF2/cation-independent mannose 6-phosphate receptor results in fetal overgrowth and perinatal lethality. Genes Dev 8: 2953-2963.
19. Gerber H, Mosser S, Boury-Jamot B, Stumpe M, Piersigilli A, et al. (2019) The APMAP interactome reveals new modulators of APP processing and beta-amyloid production that are altered in Alzheimer's disease. Acta Neuropathol Commun 7:13.
20. Borradaile NM, Han X, Harp JD, Gale SE, Ory DS, et al. (2006) Disruption of endoplasmic reticulum structure and integrity in lipotoxic cell death. J Lipid Res 47: 2726-2737.
21. Hua Y, Zhang Y, Dolence J, Shi GP, Ren J, et al. (2013) Cathepsin K knockout mitigates high-fat diet-induced cardiac hypertrophy and contractile dysfunction. Diabetes 62: 498-509.
22. Li W, Fang Q, Zhong P, Chen L, Wang L, et al. (2016) EGFR Inhibition Blocks Palmitic Acid-induced inflammation in cardiomyocytes and Prevents Hyperlipidemia-induced Cardiac Injury in Mice. Sci Rep 6: 245-280.
23. Chen X, Li H, Wang K, Liang X, Wang W, et al. (2019) Aerobic Exercise Ameliorates Myocardial Inflammation, Fibrosis and Apoptosis in High-Fat-Diet Rats by Inhibiting P2X7 Purinergic Receptors. Front Physiol 10:12-86.
24. Wang N, Ma H, Li J, Meng C, Zou J, et al. (2021) HSF1 functions as a key defender against palmitic acid-induced ferroptosis in cardiomyocytes. J Mol Cell Cardiol 150: 65-76.
25. Xu K, Liu X, Wen B, Liu Y, Zhang W, et al. (2022) A Specific Histone Lysine Demethylase 6A Inhibitor, Ameliorates Lipotoxicity to Cardiomyocytes via Preserving H3K27 Methylation and Reducing Ferroptosis. Front Cardiovasc Med 9: 907-947.
26. Wang Y, Qian Y, Fang Q, Zhong P, Li W, et al. (2017) Saturated palmitic acid induces myocardial inflammatory injuries through direct binding to TLR4 accessory protein MD2. Nat Commun 8:139-197.
27. Zheng XY, Sun CC, Liu Q, Lu XY, Fu LL, et al. (2020) Compound LM9, a novel MyD88 inhibitor, efficiently mitigates inflammatory responses and fibrosis in obesity-induced cardiomyopathy. Acta Pharmacol Sin 41: 1093-1101.
28. Yuzefovych LV, Solodushko VA, Wilson GL, Rachek LI (2012) Protection from palmitate-induced mitochondrial DNA damage prevents from mitochondrial oxidative stress, mitochondrial dysfunction, apoptosis, and impaired insulin signaling in rat L6 skeletal muscle cells. Endocrinology 153:92-100.
29. Li SN, Yu YL, Wang BY, Qiao SY, Hu MM, et al. (2022) Overexpression of G Protein-Coupled Receptor 40 Protects Obesity-Induced Cardiomyopathy Through the SIRT1/LKB1/AMPK Pathway. Hum Gene Ther 33: 598-613.
30. Li W, Ji L, Tian J, Tang W, Shan X, et al. (2021) Ophiopogonin D alleviates diabetic myocardial injuries by regulating mitochondrial dynamics. J Ethnopharmacol 271: 113-153.
31. Wen SY, Velmurugan BK, Day CH, Shen CY, Chun LC, et al. (2017) High density lipoprotein (HDL) reverses palmitic acid induced energy metabolism imbalance by switching CD36 and GLUT4 signaling pathways in cardiomyocyte. J Cell Physiol 232: 3020-3029.
32. Ren BC, Zhang YF, Liu SS, Cheng XJ, Yang X, et al. (2020) Curcumin alleviates oxidative stress and inhibits apoptosis in diabetic cardiomyopathy via Sirt1-Foxo1 and PI3K-Akt signalling pathways. J Cell Mol Med 24:12355-12367.
33. Zhou X, Chang B, Gu Y (2018) MicroRNA-21 abrogates palmitate-induced cardiomyocyte apoptosis through caspase-3/NF-kappaB signal pathways. Anatol J Cardiol 20: 336-346.
34. Galluzzi L, Vitale I, Aaronson SA, Abrams JM, Adam D, et al. (2018) Molecular mechanisms of cell death: recommendations of the Nomenclature Committee on Cell Death 2018. Cell Death Differ 25: 486-541.
35. Munier-Lehmann H, Mauxion F, Bauer U, Lobel P, Hoflack B (1996) Re-expression of the mannose 6-phosphate receptors in receptor-deficient fibroblasts. Complementary function of the two mannose 6-phosphate receptors in lysosomal enzyme targeting. J Biol Chem 271: 15166-15174.
36. Ludwig T, Ovitt CE, Bauer U, Hollinshead M, Remmler J, et al.(1993)Targeted disruption of the mouse cation-dependent mannose 6-phosphate receptor results in partial missorting of multiple lysosomal enzymes. EMBO J 12: 5225-5235.
37. Chen RJ, Wu HC, Chang MH, Lai CH, Tien YC, et al. (2000) Leu27IGF2 plays an opposite role to IGF1 to induce H9c2 cardiomyoblast cell apoptosis via Galphaq signaling. J Mol Endocrinol 43: 221-230.
38. Lai CH, Pandey S, Day CH, Ho TJ, Chen RJ, et al. (2019) beta-catenin/ LEF1/IGF-IIR Signaling Axis Galvanizes the Angiotensin-II- induced Cardiac Hypertrophy. Int J Mol Sci 20.
39. Feng CC, Pandey S, Lin CY, Shen CY, Chang RL, et al. (2018) Cardiac apoptosis induced under high glucose condition involves activation of IGF2R signaling in H9c2 cardiomyoblasts and streptozotocin-induced diabetic rat hearts. Biomed Pharmacother 97: 880-885.
40. Pandey S, Kuo WW, Shen CY, Yeh YL, Ho TJ, et al. (2019) Insulin-like growth factor II receptor-alpha is a novel stress-inducible contributor to cardiac damage underpinning doxorubicin-induced oxidative stress and perturbed mitochondrial autophagy. Am J Physiol Cell Physiol 317:235-243.
41. Chen WK, Kuo WW, Hsieh DJ, Chang HN, Pai PY, et al. (2015) CREB Negatively Regulates IGF2R Gene Expression and Downstream Pathways to Inhibit Hypoxia-Induced H9c2 Cardiomyoblast Cell Death. Int J Mol Sci 16: 27921-27930.
42. Lee SD, Chu CH, Huang EJ, Lu MC, Liu JY, et al. (2006) Roles of insulin-like growth factor II in cardiomyoblast apoptosis and in hypertensive rat heart with abdominal aorta ligation. Am J Physiol Endocrinol Metab 291: 306-314.